Biomaterials 34 (2013) 5853–5862

Contents lists available at SciVerse ScienceDirect

Biomaterials

journal homepage: www.elsevier.com/locate/biomaterials

Cardiovascular toxicity evaluation of silica nanoparticles in endothelial cells and zebrafish model

Junchao Duan [a], Yongbo Yu [a], Yang Li [b], Yang Yu [a], Zhiwei Sun [a,b,*]

[a] School of Public Health, Capital Medical University, Beijing 100069, PR China
[b] School of Public Health, Jilin University, Changchun, Jilin 130021, PR China

ARTICLE INFO

Article history:
Received 28 February 2013
Accepted 16 April 2013
Available online 8 May 2013

Keywords:
Silica nanoparticles
Cardiovascular effects
Endothelium
Zebrafish
Nanotoxicity

ABSTRACT

Environmental exposure to nanomaterials is inevitable as nanomaterials become part of our daily life, and as a result, nanotoxicity research is gaining attention. However, most investigators focus on the evaluation of overall toxicity instead of a certain organism system. In this regard, the evaluation of cardiovascular effects of silica nanoparticles was preformed in vitro and in vivo. It's worth noting that silica nanoparticles induced cytotoxicity as well as oxidative stress and apoptosis. ROS and apoptosis were considered as major factor to endothelial cells dysfunction, involved in several molecular mechanisms of cardiovascular diseases. In vivo study, mortality, malformation, heart rate and whole-embryo cellular death were measured in zebrafish embryos. Results showed that silica nanoparticles induced pericardia toxicity and caused bradycardia. We also examined the expression of cardiovascular-related proteins in embryos by western blot analysis. Silica nanoparticles inhibited the expression of p-VEGFR2 and p-ERK1/2 as well as the downregulation of MEF2C and NKX2.5, revealed that silica nanoparticles could inhibit the angiogenesis and disturb the heart formation and development. In summary, our results suggest that exposure to silica nanoparticles is a possible risk factor to cardiovascular system.

1. Introduction

Nanotechnology has been emerged as a pioneer for high-tech development in biomedical fields, most markedly in the drug delivery systems and in vivo imaging [1]. Since 2006, more than 130 nanotech-based drugs and delivery systems were in pre-clinical or clinical, as well as 125 diagnostic and imaging devices [2]. The world market for products that contain nanomaterials is expected to reach $2.6 trillion by 2015 [3]. With the development of nanotechnology, the nano-formed silica materials have gained interest for extensive applications including medical diagnostics, drug delivery, gene therapy, biomolecules detection, photodynamic therapy and bioimaging [4–6]. Silica nanomaterial is in the top five of nanomaterials explicitly referenced in nanotech-based consumer products [7]. Thus, the human exposure and environmental burden are obviously increased as the application of nanomaterials expands. Despite remarkable benefits of the power of small materials, there are open questions about how the nanoparticles used for day-to-day life may affect human health and ecological environment [8]. One of the challenges in the field of nanotechnology is environmental health and safety (EHS), which is focusing on the consideration of the properties of engineered nanomaterials (ENMs) that could pose hazards to the environment and human beings [9].

An increasing body of epidemiological evidence conducted worldwide since publication of the first American Heart Association (AHA) statement confirm the association between increased mortality and short-term elevations in $PM_{2.5}$ (particulate matter < 2.5 μm in aerodynamic diameter) that approximately equal to a 1.0% increase in daily mortality (cardiovascular death specifically) due to a 10 $\mu g/m^3$ elevation in $PM_{2.5}$ [10,11]. The overall absolute risk for mortality due to PM exposure is greater for cardiovascular than pulmonary diseases after both short- and long-term exposures [10]. Additionally, the findings indicate that short-term exposure to $PM_{2.5}$ over a period of a few hours to weeks can trigger cardiovascular-related mortality and nonfatal events, including myocardial ischemia and myocardial infarction, heart failure, arrhythmias, and strokes [10]. Although there is limited epidemiological evidence directly linking ultrafine particles (UFPs) with cardiovascular health problems, the toxicological and experimental exposure evidence is suggestive that this size fraction may pose a particularly high risk to the cardiovascular system [12,13]. Since the likelihood of cardiovascular effects and the mechanisms

* Corresponding author. School of Public Health, Capital Medical University, Beijing 100069, PR China. Tel./fax: +86 010 83911507.
E-mail address: zwsun@hotmail.com (Z. Sun).

0142-9612/$ – see front matter © 2013 Elsevier Ltd. All rights reserved.
http://dx.doi.org/10.1016/j.biomaterials.2013.04.032

triggered specifically by UFP exposure have been debated controversially, the AHA propose that future research should be explored to fully elucidate whether particles within the ultrafine size range (10–100 nm) are more harmful to the cardiovascular system or pose a relatively greater cardiovascular risk than other system [10,14].

Based on the issues above, an insight evaluation of cardiovascular effects induced by silica nanoparticles was then conducted in vitro with endothelial cells and in vivo with zebrafish model. The human umbilical vein endothelial cells (HUVECs) line isolated from the umbilical cord by collagenase digestion has been used widely for in vitro studies of endothelial cells function [15]. The pathophysiology of endothelial dysfunction is complex and involves multiple mechanisms, which is associated with several cardiovascular diseases including atherosclerosis, coronary artery disease, diabetic vasculopathy, hypertension and heart failure [16,17]. While zebrafish as a correlative and predictive model for assessing biomaterial nanotoxicity, are particular desirable in cardiovascular disease studies since the heart is the first organ to form and function during transparent embryos development [18,19]. It is also important to find ways of linking toxic effects at the in vitro level to biological injury in vivo so as to develop a predictive toxicological paradigm that maintains balance of knowledge generation at the cellular and tissue levels versus more relevant. In this regard, we evaluated the cardiovascular effects of silica nanoparticles using both in vitro and in vivo model, which may provide more persuasive evidence for nano EHS studies and AHA statements to support the hypothesis that UFPs is a possible risk factor contributing to cardiovascular morbidity and mortality. It will in turn be helpful in managing risk and providing guidance for reducing hazardous effects, and safe-by-design strategies for improving nanomaterials and nano-related products.

2. Materials and methods

2.1. Silica nanoparticles preparation and characterization

Silica nanoparticles were prepared using the Stöber method [20]. Briefly, 2.5 mL of tetraethylorthosilicate (TEOS) (Sigma, USA) was added to premixed ethanol solution (50 mL) containing ammonia (2 mL) and water (1 mL). The reaction mixture was kept at 40 °C for 12 h with continuous stirring (150 r/min). The resulting particles were isolated by centrifugation (12,000 r/min, 15 min) and washed three times with deionized water and then dispersed in 50 mL of deionized water. The size of silica nanoparticles was performed by transmission electron microscope (TEM) (JEOL JEM2100, Japan), and the size distribution was measured using ImageJ software (National Institutes of Health, USA). The hydrodynamic sizes and zeta potential of silica nanoparticles were examined by Zetasizer (Malvern Nano-ZS90, Britain). Suspensions of silica nanoparticles were dispersed by sonicator (160 W, 20 kHz, 5 min) (Bioruptor UDC-200, Belgium) before addition to culture medium in order to minimize their aggregation.

2.2. In vitro study

2.2.1. Cell culture and exposure to silica nanoparticles

The primary human umbilical vein endothelial cells (HUVECs) line was purchased from the Cell Resource Center, Shanghai Institutes for Biological Sciences (SIBS, China). The cells were maintained in Dulbecco's Modified Eagle's Medium (DMEM) (Gibco, USA) supplemented with 10% fetal bovine serum (Gibco, USA), 100 U/mL penicillin and 100 μg/mL streptomycin, and cultured at 37 °C in 5% CO_2 humidified environment. For experiments, the cells were seeded in 6-well plates (except MTT assay using 96-well plates) at a density of 1×10^5 cells/mL and allowed to attach for 24 h, then treated with silica nanoparticles (25, 50, 75 and 100 μg/mL) suspended in DMEM for 24 h. Controls were supplied with an equivalent volume of DMEM without silica nanoparticles. Each group had five replicate wells.

2.2.2. Detection of silica nanoparticles uptake

After HUVECs incubated for 24 h with silica nanoparticles (50 μg/mL), the cells were washed with PBS and then centrifuged at 2000 r/min for 10 min. The supernatants were removed. The cell pellets were fixed in a 0.1 M PBS solution containing 2.5% glutaraldehyde and 4% paraformaldehyde for 3 h. They were then washed with 0.1 M PBS, embedded in 2% agarosegel, postfixed in 4% osmium tetroxide solution for 1 h, washed with distilled water, stained with 0.5% uranyl acetate for 1 h, dehydrated in a graded series of ethanol (30%, 60%, 70%, 90%, and 100%), and embedded in epoxy resin. The resin was polymerized at 60 °C for 48 h. Ultrathin sections obtained with a ultramicrotome were stained with 5% aqueous uranyl acetate and 2% aqueous lead citrate, air dried, and imaged under a transmission electron microscope (TEM) (JEOL JEM2100, Japan).

2.2.3. MTT assay

Cultured HUVECs were treated with various concentrations (25, 50, 75 and 100 μg/mL) of silica nanoparticles for 24 h. The cell viability was measured using the 3-(4, 5-dimethylthiazol-2-yl)-2, 5-diphenyltetrazolium bromide (MTT) reduction assay. The absorbance of formazan was measured at 492 nm using a microplate reader (Themo Multiscan MK3, USA).

2.2.4. Assessment of LDH activity

Lactate dehydrogenase leakage, which is evaluated the membrane integrity damage, was determined using LDH Kit (Jiancheng, China). After HUVECs treated with different concentrations (25, 50, 75 and 100 μg/mL) of silica nanoparticles for 24 h, the supernatants were collected for LDH measurement. 100 μL cell medium was used for LDH activity analysis and the absorbance at 440 nm was measured by a UV–visible spectrophotometer (Beckman DU-640B, USA).

2.2.5. Apoptosis assay

Apoptosis in endothelial cells was measured using the Annexin V-propidium iodide (PI) apoptosis detection kit (KeyGen, China). Briefly, HUVECs were exposed to silica nanoparticles for 24 h, washed with PBS three times and trypsinized. After centrifugation at 1000 rpm, the cell pellet was washed with PBS once and incubated with 5 μL Annexin V-FITC for 15 min, which was followed by staining with 5 μL PI. Then, the samples were diluted with 500 μL binding buffer and analyzed with a flow cytometer (Becton Dickinson, USA), and at least 1×10^4 cells were counted for each sample. The cell population was gated on the basis of the forward and side-scatter properties. The different labeling patterns in the Annexin V-PI analysis identified the different cell populations where FITC negative and PI negative were designated as live cells; FITC positive and PI negative as early apoptotic cells; FITC positive and PI positive as late apoptotic cells; and FITC negative and PI positive as cells fragments.

2.2.6. Intracellular ROS measurement

The production of intracellular ROS was measured by flow cytometry using the 2′, 7′-dichlorofluorescein diacetate (DCFH-DA) (Beyotime, China) as an oxidation-sensitive probe. Briefly, 10 mM DCFH-DA stock solution was diluted 1000-fold in cell culture medium without serum or other additive to yield a 10 μM working solution. After the exposure of HUVECs to series dosages (25, 50, 75 and 100 μg/mL) of silica nanoparticles for 24 h, the cells in 6-well plates were washed twice with PBS and incubated in 2 mL working solution of DCFH-DA at 37 °C in dark for 30 min. Then the cells were washed twice with cold PBS and resuspended in the PBS for analysis. Fluorescent intensity and percentage of positive cells were measured by flow cytometry (Becton-Dickison, USA).

2.2.7. Assessment of oxidative damage

Briefly, after HUVECs exposure to different concentrations (25, 50, 75 and 100 μg/mL) of silica nanoparticles for 24 h, washed once with ice-cold PBS, and lysed in ice-cold RIPA lysis buffer containing 1 mM phenylmethylsulphonyl fluoride (PMSF) (DingGuo, China) and phosphatase inhibitor for 30 min. After centrifuging the lysates at 12,000 rpm, 4 °C for 10 min, the supernatants were collected and then measured using superoxide dismutase (SOD) kit (Jiancheng, China). The protein concentrations of these extracts were determined by performing the bicinchoninic acid (BCA) protein assay (Pierce, USA).

2.3. In vivo study

2.3.1. Zebrafish husbandry and exposure to silica nanoparticles

Zebrafish of the AB strain (wild-type, wt) were raised on a circulating aquarium system in an environmentally controlled room (28 °C, 80% humidity). The photoperiod was adjusted to a 14 h light/10 h dark cycle. The larval and adult zebrafish were fed with brine shrimp (hatched from eggs in 10 mL in 2 L salt water) daily. For experiments, fertilized eggs were collected and chosen under a stereomicroscope (Olympus SZX10, Tokyo, Japan) within 4 h post fertilization (hpf). All embryos were derived from the same spawns of eggs for statistical comparison between control and treated groups. Healthy embryos were placed in 24-well culture plates (10 embryos in 2 mL solution/well). Each group had six replicate wells. At all stages, the developing embryos and larvae were maintained at 28 °C in 30% Danieau's Solution [58 mM NaCl, 0.7 mM KCl, 0.4 mM $MgSO_4$, 0.6 mM $Ca(NO_3)_2$, 5 mM Hepes, pH 7.4]. Newly fertilized embryos were treated with silica nanoparticles (25, 50, 100 and 200 μg/mL) for 4–96 hpf. For valid experiments, fertilized eggs were obtained only from spawns with a fertilization rate higher than 90%. In all experiments, dead embryos and larvae were removed from the 24-well plates every 12 h.

2.3.2. Embryonic mortality

Zebrafish embryos exposed to silica nanoparticles (25, 50, 100 and 200 μg/mL) for 4–96 hpf were assessed for toxicity of a continuing observation period. The silica nanoparticles solutions were renewed and embryonic/larval mortality was evaluated every 24 h.

2.3.3. Embryonic malformation

During the exposure period (4–96 hpf), the photographs of embryos malformation were captured under a stereomicroscope (Olympus SZX10, Tokyo, Japan) and the percentage of abnormal embryos was counted every 24 h.

2.3.4. Heart rate assay

For heart rate studies, during the continuing exposure period (4–96 hpf), the heart rate of embryos was measured at 24 hpf and 48 hpf time point, respectively. 10 embryos of each group anesthetized in 0.016% (w/v) tricaine (ethyl 3-aminobenzoate methanesulfonate, Sigma) were counted under a stereomicroscope (SZX10, Olympus, Tokyo, Japan) for 1 min.

2.3.5. Cellular death assay

Cell death was detected in live embryos using acridine orange (AO) staining, a nucleic acid selective metachromatic dye that interacts with DNA and RNA by intercalation or electrostatic attractions [21]. AO stains cells with disturbed plasma membrane permeability so it preferentially stains necrotic or late apoptotic cells, whereas normal cells are nonpermeable to AO. Embryos were exposed to silica nanoparticles (25, 50, 100 and 200 μg/mL) for 4–28 hpf. Then embryos were rinsed three times with PBS and incubated in 5 μg/mL AO for 30 min in the dark at 28 °C, followed by three times rinses in PBS. Stained embryos were examined using fluorescence microscopy (Olympus BX61, Tokyo, Japan). Whole-embryo fluorescence was measured and quantified using Volocity Demo 6.1.1 software (PerkinElmer, USA).

2.3.6. Western blot analysis

The immunoblotting procedure has been previously described [22]. Briefly, total protein of zebrafish embryos was extracted with the Tissue Protein Rapid Extraction Kit (Keygen, China) and determined by performing the bicinchoninic acid (BCA) protein assay (Pierce, USA). The equal amounts of lysate proteins (100 μg) were loaded onto SDS-polyacrylamide gels (12% separation gels) and electrophoretically transferred to polyvinylidene fluoride (PVDF) membranes (Millipore, USA). After blocking with 5% nonfat milk in Tris-buffered saline (TBS) containing 0.05% Tween-20 (TBST) for 1 h at room temperature, the membrane was incubated with p-VEGFR2, VEGFR2, p-ERK1/2, ERK1/2, MEF2C, NKX2.5 (1:1000, rabbit antibodies, Abcam, Britain) overnight at 4 °C, washed with TBST, and incubated with a horseradish peroxidase-conjugated anti-rabbit Ig G secondary antibody (Abcam, Britain) for 1 h at room temperature. After washed three times with TBST, The antibody-bound proteins were detected using the ECL chemiluminescence reagent (Pierce, USA).

2.4. Statistical analysis

Data were expressed as mean ± S.D. and significance was determined by using one-way analysis of variance (ANOVA) followed by least significant difference (LSD) test to compare the differences between groups. Differences were considered significant at $p < 0.05$.

3. Results

3.1. Characterization of silica nanoparticles

As shown in Fig. 1A, the TEM images of silica nanoparticles had a spherical shape with the average diameter of 62 nm [23]. The size distribution was measured by ImageJ software showed approximately normal distribution (Fig. 1B). The hydrodynamic sizes of silica nanoparticles were measured in distilled water as stock media and in DMEM and 30% Danieau's Solution as culture media at different time point (Table 1). Our data showed silica nanoparticles exhibited good monodispersity in DMEM and 30% Danieau's Solution. Zeta potentials provide quantitative information on the stability of the particles. Silica nanoparticles tested in our study had the absolute value of zeta potentials is higher than 30 mV. It is well documented that the particles are more likely to remain dispersed if the absolute value of zeta potential is higher than 30 mV [24]. Our results demonstrated that the silica nanoparticles in culture medium possessed uniform shape along with relatively favorable dispersibility.

3.2. Subcellular localization of silica nanoparticles

Since the subcellular localization may play an important role in silica nanoparticles-induced biological effects, we examined the HUVECs uptake of silica nanoparticles by TEM. The images (Fig. 2) showed that the silica nanoparticles were internalized into cells [23]. Our results demonstrated that the silica nanoparticles were mainly accumulated in the perinuclear region, but did not penetrate the nucleus.

3.3. Cytotoxicity of HUVECs induced by silica nanoparticles

To evaluate the possible toxicity of silica nanoparticles on endothelial cells, cell viability and LDH activity were determined after exposing HUVECs to silica nanoparticles (25, 50, 75 and 100 μg/mL) for 6 h, 12 h and 24 h. As indicated in Fig. 3A, viability of HUVECs induced by silica nanoparticles showed no significant change as early as at 6 h. As time passed, cell viability was decreased remarkably in 75 μg/mL treated group at 12 h. Up to 24 h, the cell viability in 50 μg/mL treated group decreased to 85.49%, which was significantly lower than that of control. In addition, the MTT results were strongly in accordance with the increased membrane damage measured by LDH activity (Fig. 3B). Significant difference of LDH activity was observed between treated groups and control group after HUVECs exposure to silica nanoparticles for 6 h, 12 h and 24 h, respectively. Our results indicated that silica nanoparticles induced cytotoxicity in a dose- and time-dependent manner.

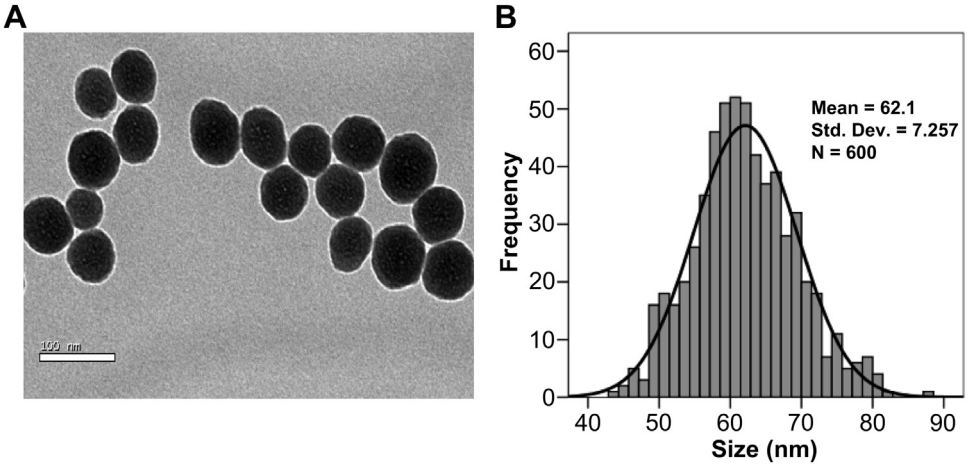

Fig. 1. Characterization of silica nanoparticles. (A) Transmission electron microscopy image. (B) Size distribution. Silica nanoparticles exhibited good monodispersity and showed approximately normal distribution.

Table 1
Hydrodynamic size and zeta potential of silica nanoparticles in dispersion media.

	Distilled water		DMEM		30% Danieau's solution	
	Diameter (nm)	Zeta potential (mV)	Diameter (nm)	Zeta potential (mV)	Diameter (nm)	Zeta potential (mV)
1 h	108.03 ± 0.61	−40.33 ± 6.47	106.03 ± 0.93	−35.27 ± 2.10	107.03 ± 0.83	−38.10 ± 2.31
3 h	106.80 ± 0.63	−39.13 ± 5.26	105.83 ± 0.90	−36.77 ± 2.40	106.83 ± 0.64	−37.97 ± 3.46
6 h	105.60 ± 1.22	−41.43 ± 3.29	107.27 ± 0.93	−36.53 ± 0.64	107.21 ± 0.61	−40.53 ± 1.64
12 h	104.97 ± 0.60	−44.10 ± 1.30	104.23 ± 1.17	−34.37 ± 2.75	105.60 ± 0.79	−44.57 ± 3.69
24 h	104.87 ± 0.64	−46.33 ± 3.13	104.43 ± 0.21	−38.10 ± 0.46	104.93 ± 0.61	−43.10 ± 2.36

Data are expressed as means ± S.D. from three independent experiments.

3.4. Apoptosis of HUVECs induced by silica nanoparticles

To further analyze the cell death caused by silica nanoparticles, apoptosis in HUVECs were measured by flow cytometry. As shown in Fig. 4, after 24 h of exposure, the total apoptotic rate was significant increased in 25 μg/mL treated group compared to that of control group. The early apoptosis rate was much lower than late apoptosis rate induced by silica nanoparticles. Our data indicated that the silica nanoparticles caused late apoptosis was mainly responsible for cell death of HUVECs.

3.5. Oxidative stress and oxidative damage triggered by silica nanoparticles

To get a closer insight into the mechanisms of silica nanoparticles on endothelial cells, we measured the generation of ROS through fluorescence intensity of dichlorofluorescein (DCF). As shown in Fig. 5A, after HUVECs exposure to silica nanoparticles for 24 h, the intracellular ROS levels of all treated groups were increased gradually. At the highest concentration (100 μg/mL), the fluorescence intensity was significantly elevated (2.5-fold much higher than that of control). The generation of intracellular ROS could cause oxidative damage. Therefore, we measured the activity of SOD in HUVECs exposed to silica nanoparticles for 24 h Fig. 5B shown that the intracellular level of SOD was significantly decreased compared to that of control group. Our results revealed that silica nanoparticles-induced ROS generation in HUVECs caused oxidative damage followed by the inhibition of SOD activity in a dose-dependent manner.

3.6. Mortality of embryos induced by silica nanoparticles

To evaluate the possible toxicity of zebrafish embryos exposure to silica nanoparticles (25, 50, 100 and 200 μg/mL), we measured the mortality in a continuing observation period. As shown in Fig. 6,

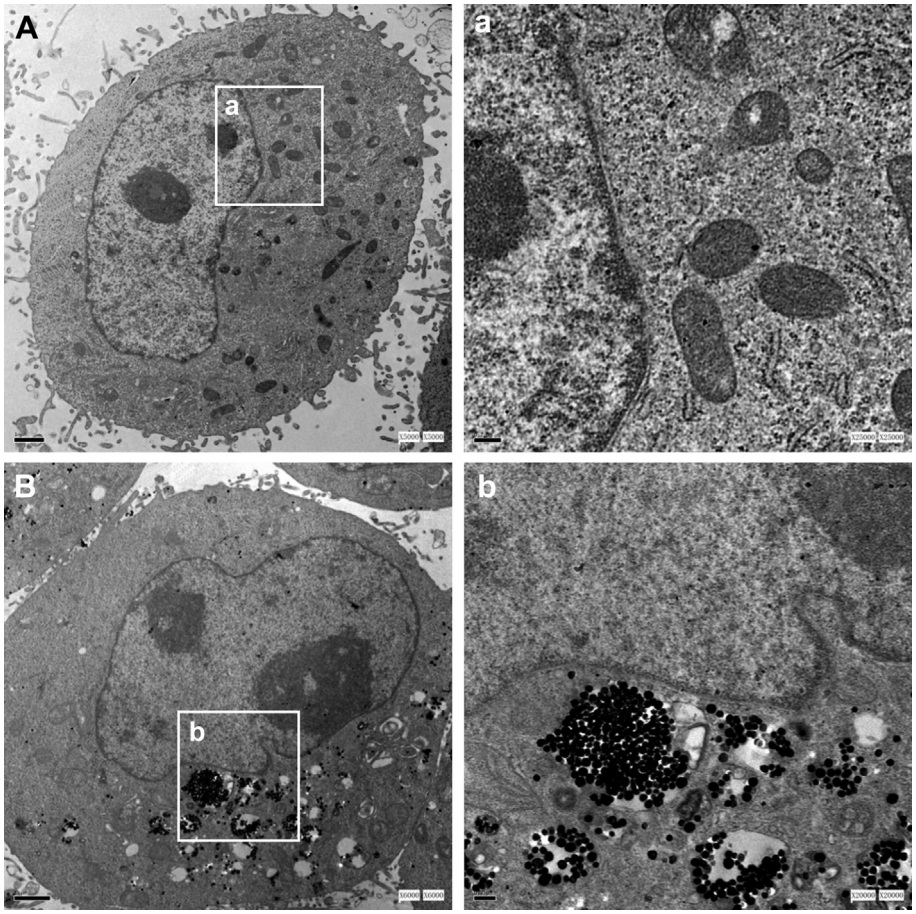

Fig. 2. TEM images of subcellular localization of silica nanoparticles. (A) Control group, (B) 50 μg/mL treated group. The silica nanoparticles were internalized into cells and was mainly accumulated in the perinuclear region.

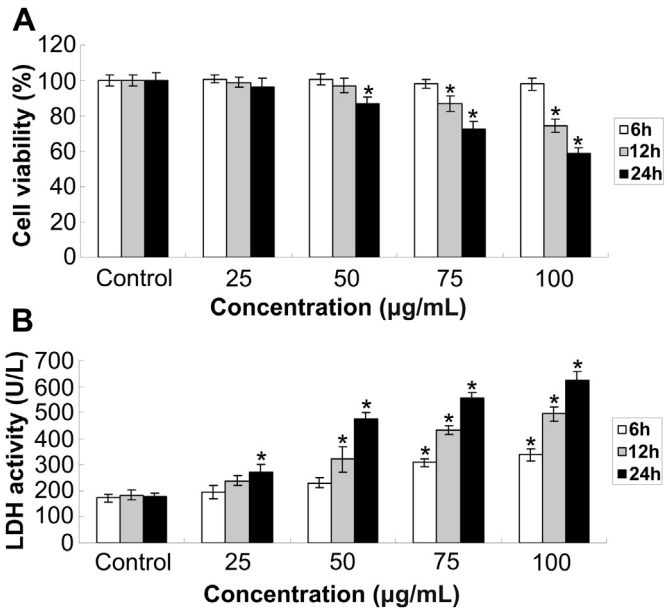

Fig. 3. Cytotoxicity of HUVECs induced by silica nanoparticles. (A) Cell viability of HUVECs treated with silica nanoparticles was measured by MTT assay after 6 h, 12 h, 24 h exposure. (B) LDH leakage of HUVECs exposed to various concentrations of silica nanoparticles for 6 h, 12 h, 24 h. Data are expressed as means ± S.D. from three independent experiments (*$p < 0.05$).

at the lower concentrations, there was no significant difference in mortality. With dosages increasing, the mortality of 100 and 200 μg/mL treated groups increased significantly compared to control group. The mortality of embryos exposed to silica nanoparticles increased in a dose- and time-dependent manner.

3.7. Malformation of embryos caused by silica nanoparticles

Representative embryonic developmental stages were imaged at segmentation (12 hpf), hatching stages (48 hpf) and fully developed larvae (96 hpf). Exposure to silica nanoparticles caused embryonic malformation, including head malformation, pericardial edema, yolk sac edema and bent tail (Fig. 7A). The incidence of embryonic morphological endpoints was observed as: Pericardia > Yolk sac > Tail > Head (Fig. 7B). Taken gather, our data indicated that exposure to silica nanoparticles caused embryonic developmental toxicity in a dose- and time-dependent manner. Pericardial and yolk sac edema were mainly typically malformation of embryos induced by silica nanoparticles.

3.8. Embryonic cell death induced by silica nanoparticles

Cellular death assays were performed to determine whether exposure to silica nanoparticles would lead to an increase in cellular death in specific cells or tissues, prior to the overt signs of toxicity reported in Fig. 7. Silica nanoparticles-exposed embryos

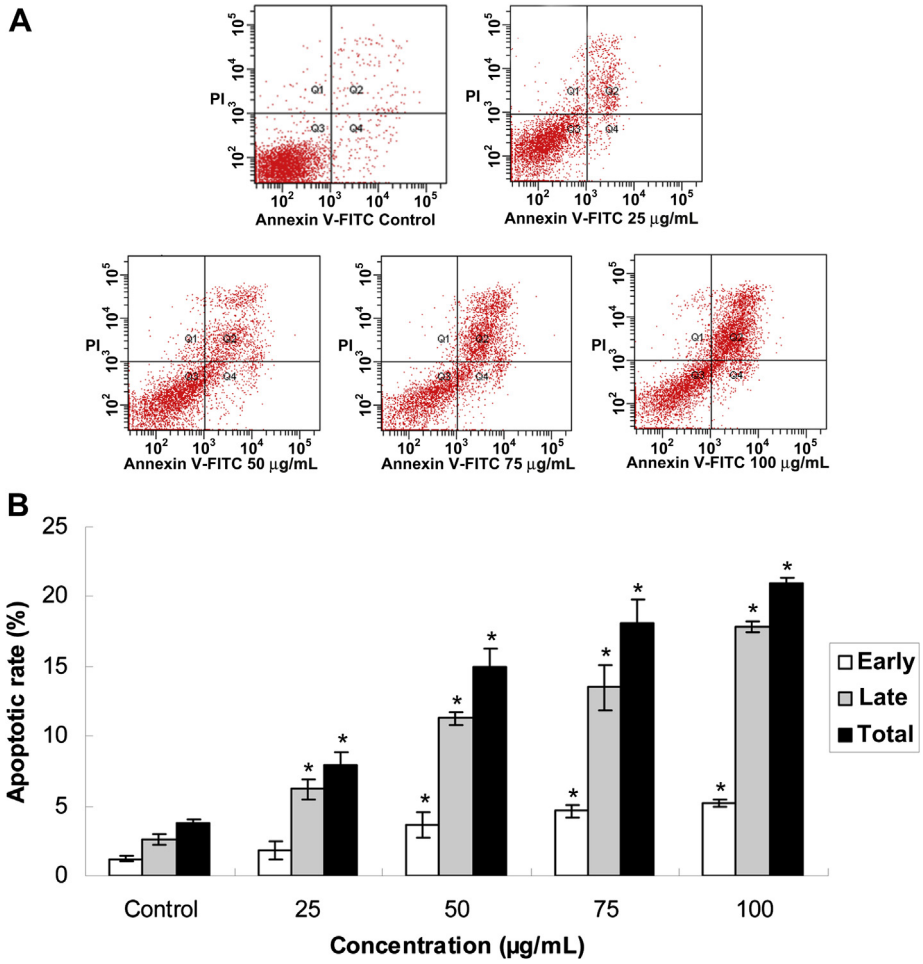

Fig. 4. Apoptosis of HUVECs after exposure to silica nanoparticles for 24 h. (A) Apoptotic populations of cells double-stained with PI- and FITC-labled Annexin V were depicted by flow cytometry. (B) HUVECs exposure to silica nanoparticles caused increase of apoptosis rate. Data are expressed as means ± S.D. from three independent experiments (*$p < 0.05$).

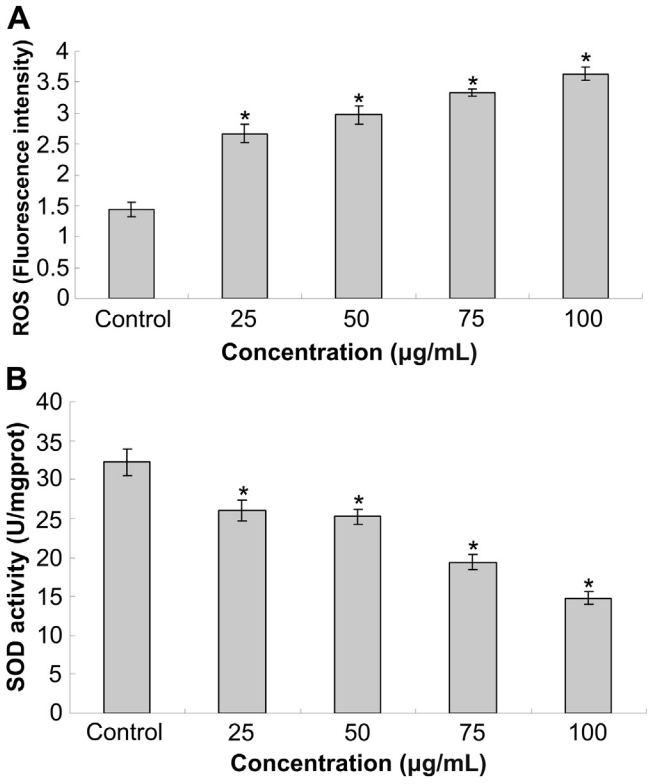

Fig. 5. Oxidative stress and oxidative damage induced by silica nanoparticles on HUVECs. The intracellular level of ROS was obviously increased (A). While SOD level was decreased significantly with a dose-dependent way (B). Data are expressed as means ± S.D. from three independent experiments (*$p < 0.05$).

exhibited a dose-dependent increase in overall cellular death, significant at higher concentrations (100 and 200 μg/mL) (Fig. 8). The distribution of death cells was mainly gathered in the head region, pericardia region and down the notochord to the region of tail. Our data showed that the relative fluorescence of cell death was detected as: Pericardia > Tail > Head. The whole-embryo fluorescence analysis was confirmed with the incidence of malformation results, showed that pericardia region was more sensitive to silica nanoparticles than other regions.

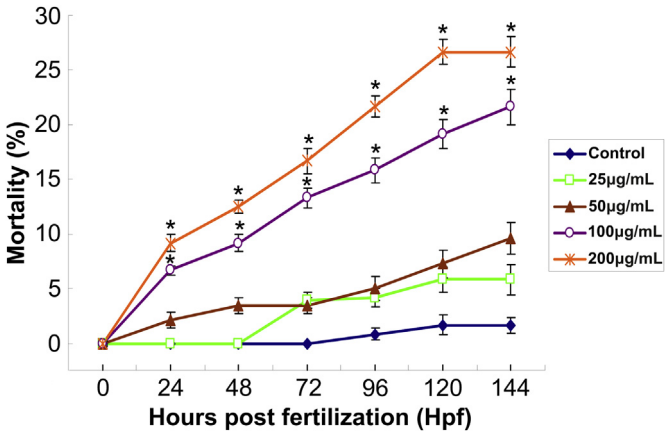

Fig. 6. Mortality of zebrafish embryos exposed to silica nanoparticles. The mortality of embryos increased in dose- and time-dependent manner. Data are expressed as means ± S.D. from three independent experiments (*$p < 0.05$).

3.9. Cardiac effects of silica nanoparticles

We examined the heart rate of embryos exposed to silica nanoparticles (25, 50, 100 and 200 μg/mL) at 24 hpf and 48 hpf time point, respectively. As shown in Fig. 9, the heart rate decreased in a dose- and time-dependent manner. At the highest concentration (200 μg/mL), the heart rate of embryos was 68 beats/min compared to 90 beats/min of control at 24 hpf. Up to 48 hpf, the heart rate was 122 beats/min much lower than that of control (157 beats/min). The results revealed that exposure to silica nanoparticles caused embryos bradycardia and may lead to arrhythmias.

3.10. Cardiovascular effects of silica nanoparticles in zebrafish embryos

To better understand the mechanisms of cardiovascular effects of silica nanoparticles in zebrafish embryos, we examined the expression of cardiovascular-related proteins by western blot analysis. As shown in Fig. 10, the expression of vascular endothelial growth factor receptor 2 (VEGFR2) had no significant change after embryos exposed to silica nanoparticles for 4–96 hpf, whereas the expression of phosphorylated VEGFR2 was marked inhibited in a dose-dependent way. The expression of angiogenesis-related ERK1/2 was decreased progressively and the phosphorylated ERK1/2 was obviously inhibited. MEF2C, the key factor of vertebrate anterior heart field development, was inhibited remarkably. NKX2.5, which is required for heart morphogenesis and maturation, was decreased gradually. Our data demonstrated that silica nanoparticles inhibited the angiogenesis and disturbed the heart formation and development in zebrafish embryos.

4. Discussion

Environmental exposure to nanomaterials is inevitable as nanomaterials become part of our daily life. Therefore, nanotoxicity research is gaining attention. In the present study, we demonstrated for the first time evaluating the cardiovascular effects and mechanisms of silica nanoparticles using both in vitro and in vivo, which may provide more persuasive evidence for nano EHS studies and support the hypothesis proposed by AHA that the particles within the ultrafine size range (10–100 nm) are more harmful to the cardiovascular system or pose a relatively greater cardiovascular risk than other system.

Currently, cellular uptake of nanoparticles is an important issue in designing suitable cell-tracking and drug-carrier nanomaterials systems [25]. Therefore, we first examined the cellular uptake of silica nanoparticles. TEM images showed that the internalization and perinuclear localization of silica nanoparticles occurred after 24 h exposure (Fig. 2). In general, it is known that there is a correlation between size and cellular uptake of nanoparticles. Earlier studies suggested that the maximum uptake by cells occurred at an average size of 50 nm nanoparticles [26,27]. Similar with our results, Bauer and coworkers showed that silica nanoparticles with a size of 310 nm accumulated around the nucleus, suggested the perinuclear localization is associated with cell death [28]. To gain a closer insight into silica nanoparticles induced biological effects on endothelial cells, cell viability and membrane integrity were measured as indicators of cytotoxicity. Our data demonstrated that silica nanoparticles induced cytotoxicity increased in a dose- and time-dependent manner (Fig. 3). MTT assay is the most common employed for the detection of cytotoxicity or cell viability following exposure to toxic substances. The LDH release, which is based on the measurement of lactate dehydrogenase activity in the extracellular medium, is an indicator of irreversible cell death due to cell membrane damage.

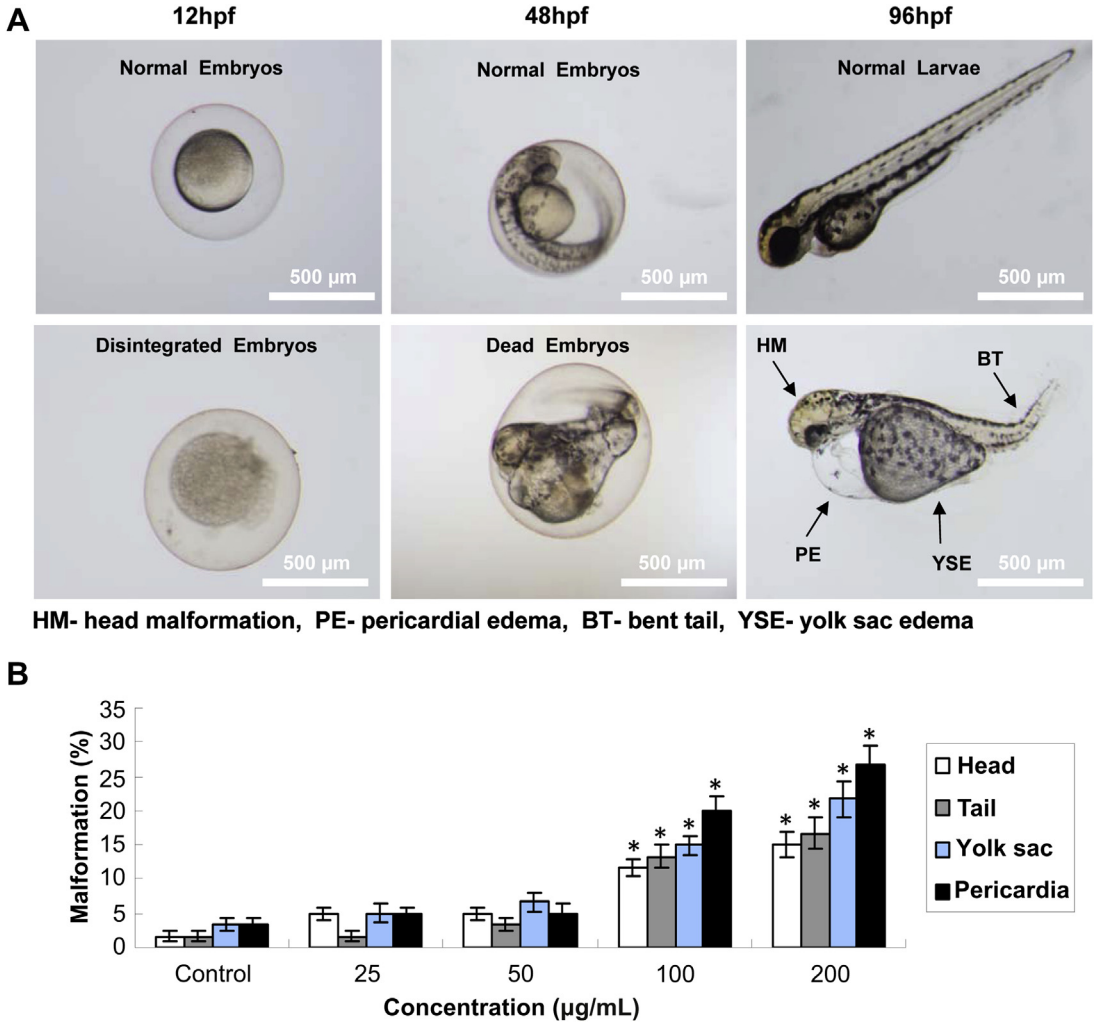

Fig. 7. Malformation of zebrafish embryos exposed to silica nanoparticles. (A) Representative optical images of deformed zebrafish at 12, 48, 96 hpf time point. (B) Pericardial and yolk sac edema were mainly typically malformation of embryos induced by silica nanoparticles. Data are expressed as means ± S.D. from three independent experiments ($^*p < 0.05$).

To further analyze the cell death caused by silica nanoparticles, apoptosis in HUVECs were measured by flow cytometry (Fig. 4A). Our data showed that the apoptosis rate increased remarkable compared to control group (Fig. 4B). Similar results were obtained from Liu and coworker who suggested that the endothelial cells exposure to silica nanoparticles could cause apoptosis [29]. Endothelial cells apoptosis could lead to endothelial cells dysfunction and was considered as a major determinant of atherothrombosis [30]. Atherosclerosis is a key pathological basis for cardiovascular diseases such as ischemic heart disease and stroke [31]. Apoptosis is a slow-acting form of cell death accompanied with an energy-dependent sequence of events, resulted in fragmenting nuclei and cytoplasmic organelles ultimately, thus, the membrane damage is not a primary event of apoptosis [32]. To investigate the possible mechanisms of apoptosis induced by silica nanoparticles, intracellular ROS and antioxidant activity of SOD were measured. Our results showed that the generation of intracellular ROS caused oxidative damage followed the inhibition of antioxidant activity (Fig. 5). Induction of oxidative stress by silica nanoparticles has been observed in various cell types [33–35]. Oxidative stress is the result of an imbalance in the pro-oxidant/antioxidant homeostasis. Findings suggested that oxidative excess could reduce NO bioavailability and lead to endothelial dysfunction, involved in the impairment of endothelium-dependent vasodilation [36,37]. In addition, clinical studies demonstrated that the presence of impaired endothelium-dependent vasodilation was an independent predictor of future cardiovascular morbidity and mortality [38,39].

It is a fairly simple and cost-effective method to initially screen the toxicity of nanomaterials by in vitro cell cultures. However, it is difficult to imitate a complimentary in vivo system. Alternatively, the millimeter-sized zebrafish are proving to be a quick and facile model to conservatively assess toxicity of nanomaterials in vivo [18]. It was well documented that earlier developmental embryos are more sensitive to external substances than larval or adult zebrafish [40]. Therefore, the embryonic period (4–96 hpf) was chosen as administration time to study the possible toxicity of silica nanoparticles. In the present study, our data showed that exposure to silica nanoparticles caused the increasing of mortality in a dose- and time-dependent manner (Fig. 6). Consistent with our findings, decreasing survival of zebrafish embryos have been observed in various nanomaterials [41–43]. It's worth noting that the mortality of embryos at 96 hpf (the ending exposure time point) was only 21.7% in the highest treated group, which was much lower than the median lethal dose, LD_{50}. However, the cardiovascular effects of silica nanoparticles on embryos were observed obviously in several

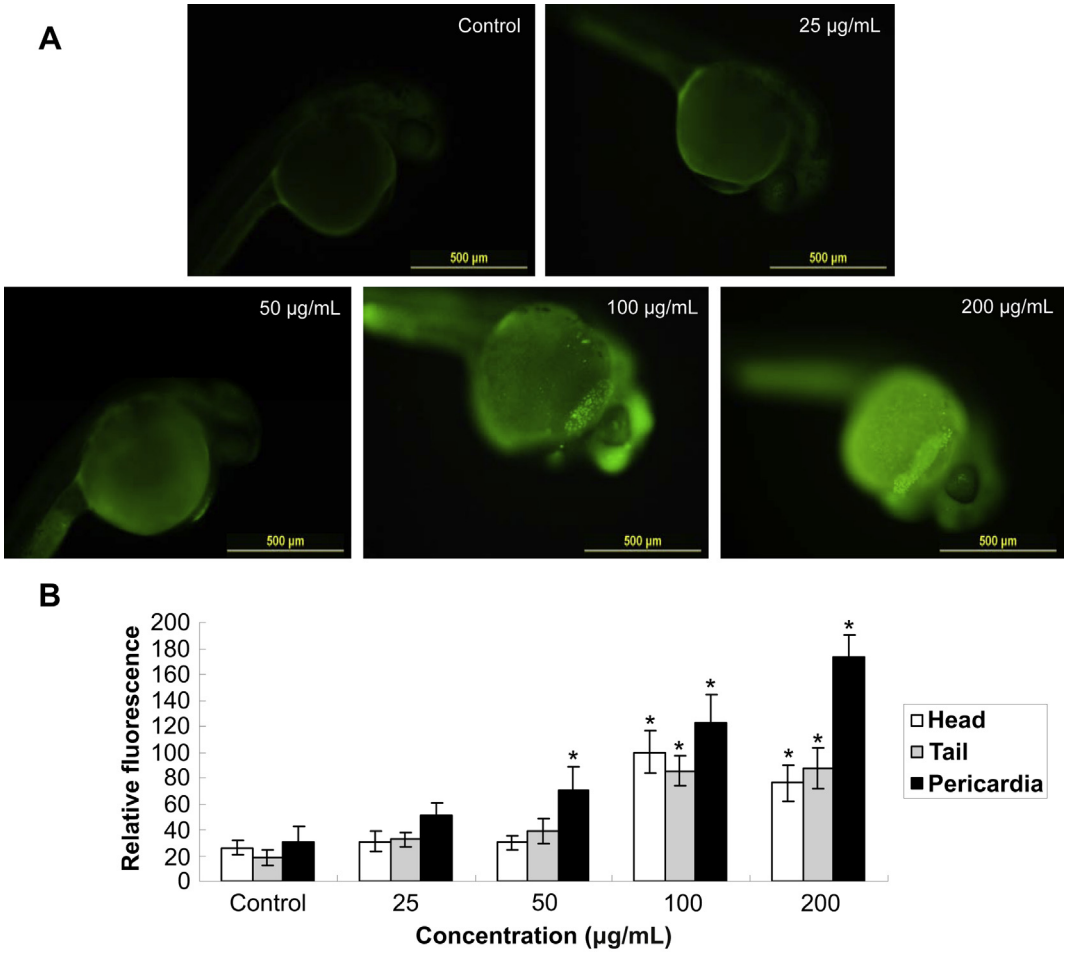

Fig. 8. Cellular death was determined using acridine orange staining of silica nanoparticles-exposed embyos at 28 hpf, after a 24 h exposure. (A) Whole-embryo cell death images were detected by fluorescence microscope. (B) The relative fluorescence of cell death was detected as: Pericardia > Tail > Head. Data are expressed as means ± S.D. from three independent experiments (*$p < 0.05$).

indicators, such as malformation, whole-embryo cell death, heart rate and the expression of cardiovascular-related proteins.

From in vivo study, we observed several types of malformation in embryos incubating with silica nanoparticles (25, 50, 100 and 200 μg/mL), including pericardial edema, head malformation, yolk sac edema and bent tail (Fig. 7A). The results in Fig. 7B showed that the pericardial edema and yolk sac edema occurred as common malformations observed in embryos exposed to silica nanoparticles. Similar with our results, Xu and coworkers reported that serious yolk sac edema and pericardial edema were found in embryos treated with titanium dioxide nanoparticles, suggesting that titanium dioxide nanoparticles may have a toxic effect on cardiovascular system [44]. While fin fold and tail abnormalities were observed as the most common ones when embryos incubating with sliver nanoparticles [45]. Thus, we could also confirm that different nanomaterials led to different types of malformations

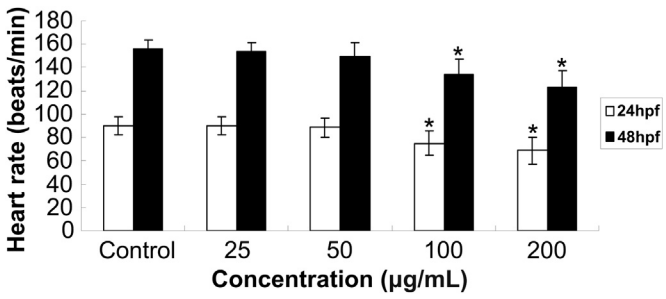

Fig. 9. Heart rate of zebrafish embryos exposed to silica nanoparticles at 24 hpf and 48 hpf. Embryos treated with silica nanoparticles had significant bradycardia at 100 and 200 μg/mL groups. Data are expressed as means ± S.D. from three independent experiments (*$p < 0.05$).

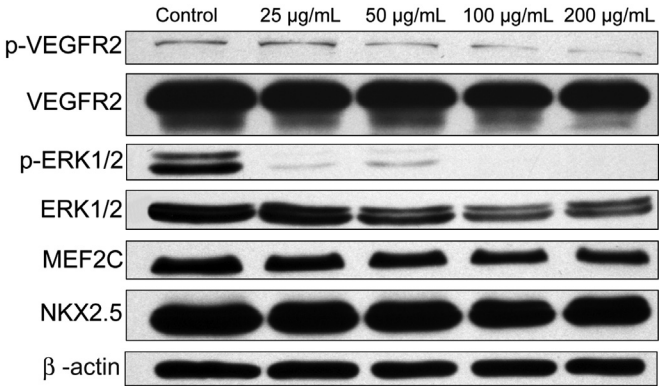

Fig. 10. Cardiovascular effects of silica nanoparticles on the early developing zebrafish embryos. The expression of p-VEGFR2, VEGFR2, p-ERK1/2, ERK1/2, MEF2C and NKX2.5 was measured by western blot analysis. Silica nanoparticles inhibited the expression of p-VEGR2 and p-ERK1/2, as well as downregulated the expression of MEF2C and NKX2.5. β-actin was used as an internal control to monitor for equal loading.

in zebrafish embryos. To better understand the overt signs of malformation reported in Fig. 7, cellular death assays were performed by AO staining (Fig. 8A). Fig. 8B showed that exposure to silica nanoparticles for 24 h led to an increase in cellular death in specific region: Pericardia > Tail > Head. AO binds all cells undergoing cellular death, both necrosis and apoptosis [21]. In addition, the mechanism of cellular death induction is an important consideration because of its correlation with overall tissue damage: Necrosis tends to cause extensive tissue damage resulting in an inflammatory response in vivo; while apoptosis does not cause tissue damage since macrophages effectively remove apoptotic signaling cells [46]. AO staining for cellular death, as a sensitive endpoint prior the overt signs of malformation, showed that more death of cells occurred in pericardia than other regions, which indicated that silica nanoparticles may have a toxic effect on zebrafish heart. Therefore, we determined the heart rate to analyze whether the exposure of silica nanoparticles could impact on embryos cardiac function. The heart tissue is the first organ to form and function in the zebrafish embryos [19]. Due to the embryo's transparency, heart development, heart rate analysis and phenotypic characterization can be studied at single-cell resolution [47]. In addition, the heart rate is an important indicator as assessment of embryos cardiac function [48]. An earlier study reported that malformed hearts was observed in embryos exposed to quantum dots [49]. In this study, we quantified the heart rate under a stereomicroscope for 1 min (Fig. 9). Our data showed that exposure to silica nanoparticles caused heart rate decreased in a dose- and time-dependent manner, indicated that silica nanoparticles could impact on cardiac function, cause embryos bradycardia and may lead to arrhythmias.

To gain an insight into the mechanisms of cardiovascular effects of silica nanoparticles in zebrafish embryos, we examined the expression of cardiovascular-related proteins by western blot analysis (Fig. 10). Vascular endothelial growth factor (VEGF) exerts its biological effects by binding to its receptor tyrosine kinases, expressed on endothelial cells [50]. The biologically relevant VEGF signaling events are mediated mainly via VEGFR2 [51]. Activation of VEGFR2 leads to the activation of downstream signal transduction protein, extracellular signal-related kinase (ERK), which promotes the growth, migration, differentiation and survival of endothelial cells in preexisting vasculature [52]. The myocyte enhancer factor 2 (MEF2) family has been strongly linked with early heart development [53]. MEF2C, as a member of the MEF2 family, is a key cardiomyogenic regulator expressed in heart precursor cells prior to linear heart tube formation [54,55]. Targeted disruption of MEF2C in the mouse leads to early embryonic lethality associated with cardiac looping defect and absence of the right ventricle [56]. NK2 transcription factor-related 5 (NKX2.5), as an early precardiac marker, play an important role in cardiac progenitor specification [57]. Patients diagnosed with Nkx2.5 haploinsufficiencies exhibit several progressive heart defects, including atrial and ventricular septal defects and atrioventricular conduction system abnormalities [58–60]. Our data showed that silica nanoparticles inhibited the expression of p-VEGR2 and p-ERK1/2, as well as downregulated the expression of MEF2C and NKX2.5, suggesting that silica nanoparticles could inhibit the angiogenesis and disturb the heart formation and development in zebrafish embryos. Antiangiogenesis is associated with various cardiovascular diseases, including ischemic heart disease (IHD), ischemic limb disease (IHD) and peripheral vascular diseases [61]. Cardiovascular ischemia is the leading cause of morbidity and mortality in the Western as well as developing countries [62]. The molecular mechanism obtained from our study may add information to the hypothesis proposed by AHA that exposure to UFPs is a possible risk factor to the cardiovascular system. It also should be noted that this study was conducted in an ideal experimental system, there are much complicated in ecosystem.

5. Conclusions

In the present study, using both in vitro and in vivo assays, we showed that: (1) Silica nanoparticles induced endothelial cells dysfunction via oxidative stress and apoptosis. (2) Silica nanoparticles caused embryonic toxicity and cardiovascular effects in early developing zebrafish embryos. (3) The mechanism of cardiovascular effects in zebrafish embryos induced by silica nanoparticles was through inhibiting the angiogenesis and disturbing the heart formation and development. Thus, our findings suggest that exposure to silica nanoparticles could be a potential hazardous factor to the cardiovascular system, more studies of relation between silica nanoparticles exposure, adverse effects and biological mechanisms are needed for the safety evaluation and biomedical application of nanoparticles.

Acknowledgments

The authors would like to thank to Prof. Wensheng Yang from Jilin University for the preparation of silica nanoparticles. The authors would also like to thank to Prof. Shuangqing Peng from Academy of Military Medical Sciences for technical support. This work was supported by National Natural Science Foundation of China (no. 81230065, no. 81172704), Funding Project for Academic Human Resources Development of Beijing Education Committee (PHR201006110) and Innovative Team Project of Beijing Education Committee (PHR201107116).

References

[1] Service RF. Nanotoxicology. Nanotechnology grows up. Science 2004;304:1732–4.
[2] Maynard AD. A research strategy for addressing risk. Nanotechnology. Woodrow Wilson International Center for Scholars; 2006.
[3] United States Government Accountability Office report on nanotechnology: nanomaterials are widely used in commerce, but EPA faces challenges in regulating risk. Int J Occup Environ Health 2010;16:525–39.
[4] Qian J, Wang D, Cai F, Zhan Q, Wang Y, He S. Photosensitizer encapsulated organically modified silica nanoparticles for direct two-photon photodynamic therapy and in vivo functional imaging. Biomaterials 2012;33:4851–60.
[5] Li Z, Barnes JC, Bosoy A, Stoddart JF, Zink JI. Mesoporous silica nanoparticles in biomedical applications. Chem Soc Rev 2012;41:2590–605.
[6] Lee JE, Lee N, Kim T, Kim J, Hyeon T. Multifunctional mesoporous silica nanocomposite nanoparticles for theranostic applications. Acc Chem Res 2011;44:893–902.
[7] Park MV, Verharen HW, Zwart E, Hernandez LG, van Benthem J, Elsaesser A, et al. Genotoxicity evaluation of amorphous silica nanoparticles of different sizes using the micronucleus and the plasmid lacZ gene mutation assay. Nanotoxicology 2011;5:168–81.
[8] Ray PC, Yu H, Fu PP. Toxicity and environmental risks of nanomaterials: challenges and future needs. J Environ Sci Health C Environ Carcinog Ecotoxicol Rev 2009;27:1–35.
[9] Thomas CR, George S, Horst AM, Ji Z, Miller RJ, Peralta-Videa JR, et al. Nanomaterials in the environment: from materials to high-throughput screening to organisms. ACS Nano 2011;5:13–20.
[10] Brook RD, Rajagopalan S, Pope 3rd CA, Brook JR, Bhatnagar A, Diez-Roux AV, et al. Particulate matter air pollution and cardiovascular disease: an update to the scientific statement from the American Heart Association. Circulation 2010;121:2331–78.
[11] Pope 3rd CA, Burnett RT, Thurston GD, Thun MJ, Calle EE, Krewski D, et al. Cardiovascular mortality and long-term exposure to particulate air pollution: epidemiological evidence of general pathophysiological pathways of disease. Circulation 2004;109:71–7.
[12] Schneider A, Hampel R, Ibald-Mulli A, Zareba W, Schmidt G, Schneider R, et al. Changes in deceleration capacity of heart rate and heart rate variability induced by ambient air pollution in individuals with coronary artery disease. Part Fibre Toxicol 2010;7:29.
[13] Napierska D, Thomassen LC, Rabolli V, Lison D, Gonzalez L, Kirsch-Volders M, et al. Size-dependent cytotoxicity of monodisperse silica nanoparticles in human endothelial cells. Small 2009;5:846–53.

[14] Knol AB, de Hartog JJ, Boogaard H, Slottje P, van der Sluijs JP, Lebret E, et al. Expert elicitation on ultrafine particles: likelihood of health effects and causal pathways. Part Fibre Toxicol 2009;6:19.
[15] Kadam SS, Tiwari S, Bhonde RR. Simultaneous isolation of vascular endothelial cells and mesenchymal stem cells from the human umbilical cord. In Vitro Cell Dev Biol Anim 2009;45:23–7.
[16] Alom-Ruiz SP, Anilkumar N, Shah AM. Reactive oxygen species and endothelial activation. Antioxid Redox Signal 2008;10:1089–100.
[17] Xu F, Sun Y, Chen Y, Li R, Liu C, Zhang C, et al. Endothelial cell apoptosis is responsible for the formation of coronary thrombotic atherosclerotic plaques. Tohoku J Exp Med 2009;218:25–33.
[18] Fako VE, Furgeson DY. Zebrafish as a correlative and predictive model for assessing biomaterial nanotoxicity. Adv Drug Deliv Rev 2009;61:478–86.
[19] Bakkers J. Zebrafish as a model to study cardiac development and human cardiac disease. Cardiovasc Res 2011;91:279–88.
[20] Sun L, Li Y, Liu X, Jin M, Zhang L, Du Z, et al. Cytotoxicity and mitochondrial damage caused by silica nanoparticles. Toxicol In Vitro 2011;25:1619–29.
[21] Hu YL, Qi W, Han F, Shao JZ, Gao JQ. Toxicity evaluation of biodegradable chitosan nanoparticles using a zebrafish embryo model. Int J Nanomedicine 2011;6:3351–9.
[22] Hu Z, Zhang J, Zhang Q. Expression pattern and functions of autophagy-related gene atg5 in zebrafish organogenesis. Autophagy 2011;7:1514–27.
[23] Duan JC, Yu YB, Li Y, Yu Y, Li YB, Zhou XQ, et al. Toxic effect of silica nanoparticles on endothelial cells through DNA damage response via Chk1-dependent G2/M checkpoint. PLoS One 2013;8:e62087.
[24] Jiang J, Oberdörster G, Biswas P. Characterization of size, surface charge, and agglomeration state of nanoparticle dispersions for toxicological studies. J Nanoparticle Res 2009;11:77–89.
[25] Smith AM, Duan H, Mohs AM, Nie S. Bioconjugated quantum dots for in vivo molecular and cellular imaging. Adv Drug Deliv Rev 2008;60:1226–40.
[26] Lu F, Wu SH, Hung Y, Mou CY. Size effect on cell uptake in well-suspended, uniform mesoporous silica nanoparticles. Small 2009;5:1408–13.
[27] Chithrani BD, Ghazani AA, Chan WC. Determining the size and shape dependence of gold nanoparticle uptake into mammalian cells. Nano Lett 2006;6:662–8.
[28] Bauer AT, Strozyk EA, Gorzelanny C, Westerhausen C, Desch A, Schneider MF, et al. Cytotoxicity of silica nanoparticles through exocytosis of von Willebrand factor and necrotic cell death in primary human endothelial cells. Biomaterials 2011;32:8385–93.
[29] Liu X, Sun J. Endothelial cells dysfunction induced by silica nanoparticles through oxidative stress via JNK/P53 and NF-kappaB pathways. Biomaterials 2010;31:8198–209.
[30] Tedgui A, Mallat Z. Apoptosis, a major determinant of atherothrombosis. Arch Mal Coeur Vaiss 2003;96:671–5.
[31] Hirase T, Node K. Endothelial dysfunction as a cellular mechanism for vascular failure. Am J Physiol Heart Circ Physiol 2012;302:H499–505.
[32] Inayat-Hussain SH, Chan KM, Rajab NF, Din LB, Chow SC, Kizilors A, et al. Goniothalamin-induced oxidative stress, DNA damage and apoptosis via caspase-2 independent and Bcl-2 independent pathways in Jurkat T-cells. Toxicol Lett 2010;193:108–14.
[33] Zhang Y, Hu L, Yu D, Gao C. Influence of silica particle internalization on adhesion and migration of human dermal fibroblasts. Biomaterials 2010;31:8465–74.
[34] Choi SJ, Oh JM, Choy JH. Toxicological effects of inorganic nanoparticles on human lung cancer A549 cells. J Inorg Biochem 2009;103:463–71.
[35] Li Y, Sun L, Jin M, Du Z, Liu X, Guo C, et al. Size-dependent cytotoxicity of amorphous silica nanoparticles in human hepatoma HepG2 cells. Toxicol In Vitro 2011;25:1343–52.
[36] Heitzer T, Schlinzig T, Krohn K, Meinertz T, Munzel T. Endothelial dysfunction, oxidative stress, and risk of cardiovascular events in patients with coronary artery disease. Circulation 2001;104:2673–8.
[37] Corbalan JJ, Medina C, Jacoby A, Malinski T, Radomski MW. Amorphous silica nanoparticles trigger nitric oxide/peroxynitrite imbalance in human endothelial cells: inflammatory and cytotoxic effects. Int J Nanomedicine 2011;6:2821–35.
[38] Fichtlscherer S, Breuer S, Zeiher AM. Prognostic value of systemic endothelial dysfunction in patients with acute coronary syndromes: further evidence for the existence of the “vulnerable” patient. Circulation 2004;110:1926–32.
[39] Schachinger V, Britten MB, Zeiher AM. Prognostic impact of coronary vasodilator dysfunction on adverse long-term outcome of coronary heart disease. Circulation 2000;101:1899–906.
[40] Yan H, Teh C, Sreejith S, Zhu L, Kwok A, Fang W, et al. Functional mesoporous silica nanoparticles for photothermal-controlled drug delivery in vivo. Angew Chem Int Ed Engl 2012;51:8373–7.
[41] Bar-Ilan O, Louis KM, Yang SP, Pedersen JA, Hamers RJ, Peterson RE, et al. Titanium dioxide nanoparticles produce phototoxicity in the developing zebrafish. Nanotoxicology 2012;6:670–9.
[42] Zhu X, Zhu L, Duan Z, Qi R, Li Y, Lang Y. Comparative toxicity of several metal oxide nanoparticle aqueous suspensions to Zebrafish (Danio rerio) early developmental stage. J Environ Sci Health Part A 2008;43:278–84.
[43] Lee KJ, Nallathamby PD, Browning LM, Desai T, Cherukuri PK, Xu XH. Single nanoparticle spectroscopy for real-time in vivo quantitative analysis of transport and toxicity of single nanoparticles in single embryos. Analyst 2012;137:2973–86.
[44] Xu Z, Zhang YL, Song C, Wu LL, Gao HW. Interactions of hydroxyapatite with proteins and its toxicological effect to zebrafish embryos development. PLoS One 2012;7:e32818.
[45] Lee KJ, Browning LM, Nallathamby PD, Desai T, Cherukuri PK, Xu XH. In vivo quantitative study of sized-dependent transport and toxicity of single silver nanoparticles using zebrafish embryos. Chem Res Toxicol 2012;25:1029–46.
[46] Usenko CY, Harper SL, Tanguay RL. In vivo evaluation of carbon fullerene toxicity using embryonic zebrafish. Carbon N Y 2007;45:1891–8.
[47] Verkerk AO, Remme CA. Zebrafish: a novel research tool for cardiac (patho) electrophysiology and ion channel disorders. Front Physiol 2012;3:255.
[48] Hecker L, Khait L, Sessions SK, Birla RK. Functional evaluation of isolated zebrafish hearts. Zebrafish 2008;5:319–22.
[49] King-Heiden TC, Wiecinski PN, Mangham AN, Metz KM, Nesbit D, Pedersen JA, et al. Quantum dot nanotoxicity assessment using the zebrafish embryo. Environ Sci Technol 2009;43:1605–11.
[50] Pratheeshkumar P, Son YO, Budhraja A, Wang X, Ding S, Wang L, et al. Luteolin inhibits human prostate tumor growth by suppressing vascular endothelial growth factor receptor 2-mediated angiogenesis. PLoS One 2012;7:e52279.
[51] Ferrara N, Gerber HP, LeCouter J. The biology of VEGF and its receptors. Nat Med 2003;9:669–76.
[52] Cho CH, Lee CS, Chang M, Jang IH, Kim SJ, Hwang I, et al. Localization of VEGFR-2 and PLD2 in endothelial caveolae is involved in VEGF-induced phosphorylation of MEK and ERK. Am J Physiol Heart Circ Physiol 2004;286:H1881–8.
[53] Hinits Y, Pan L, Walker C, Dowd J, Moens CB, Hughes SM. Zebrafish Mef2ca and Mef2cb are essential for both first and second heart field cardiomyocyte differentiation. Dev Biol 2012;369:199–210.
[54] Ghosh TK, Song FF, Packham EA, Buxton S, Robinson TE, Ronksley J, et al. Physical interaction between TBX5 and MEF2C is required for early heart development. Mol Cell Biol 2009;29:2205–18.
[55] Illi B, Scopece A, Nanni S, Farsetti A, Morgante L, Biglioli P, et al. Epigenetic histone modification and cardiovascular lineage programming in mouse embryonic stem cells exposed to laminar shear stress. Circ Res 2005;96:501–8.
[56] Lin Q, Schwarz J, Bucana C, Olson EN. Control of mouse cardiac morphogenesis and myogenesis by transcription factor MEF2C. Science 1997;276:1404–7.
[57] Targoff KL, Schell T, Yelon D. Nkx genes regulate heart tube extension and exert differential effects on ventricular and atrial cell number. Dev Biol 2008;322:314–21.
[58] Jay PY, Berul CI, Tanaka M, Ishii M, Kurachi Y, Izumo S. Cardiac conduction and arrhythmia: insights from Nkx2.5 mutations in mouse and humans. Novartis Found Symp 2003;250:227–38.
[59] Blaschke RJ, Hahurij ND, Kuijper S, Just S, Wisse LJ, Deissler K, et al. Targeted mutation reveals essential functions of the homeodomain transcription factor Shox2 in sinoatrial and pacemaking development. Circulation 2007;115:1830–8.
[60] Schott JJ, Benson DW, Basson CT, Pease W, Silberbach GM, Moak JP, et al. Congenital heart disease caused by mutations in the transcription factor NKX2-5. Science 1998;281:108–11.
[61] Patra CR, Kim JH, Pramanik K, d'Uscio LV, Patra S, Pal K, et al. Reactive oxygen species driven angiogenesis by inorganic nanorods. Nano Lett 2011;11:4932–8.
[62] Yusuf S, Reddy S, Ôunpuu S, Anand S. Global burden of cardiovascular diseases. Circulation 2001;104:2855–64.